CHAPTER III

MICROGRID VOLTAGE STABILITY INDICES IMPROVEMENT USING PARTICLE SWARM OPTIMIZATION

3.1 Introduction

In section 2.2, voltage stability was presented. When the system integrates with renewable energy, it is evident that renewable energy affects the power system, especially in terms of voltage. Therefore, tools for monitoring the system's voltage stability are necessary to assess its stability. In section 2.4, a tool for evaluating VS is proposed, which is VSI. There are various VSIs used differently in this study, the L-index is presented because its calculation is not complex. It is suitable for rapid monitoring as it can compute using data from load flow analysis directly.

In this study, L-index values are used to detect the weakest buses in the electrical power system, with lower values suggesting better voltage stability. Each load bus is assigned a unique L-index depending on the power network's admittance characteristics. Using PSO, the ideal generator voltage that minimizes the L-index value is found. Finally, PV curves for the system's weakest buses are created to assess overall system performance.

3.2 L-index

The L-index predicts the occurrence of electrical collapse and provides a simple method for calculating and identifying weak buses in the power system. As a result, it is an adaptable tool for increasing system stability. The L-index is computed using the following equation:

$$I_{bus} = Y_{bus} V_{bus} \tag{3.1}$$

Furthermore, since the system comprises multiple buses, they can be incorporated into a matrix representation.

$$\begin{bmatrix} \mathbf{I^G} \\ \mathbf{I^L} \end{bmatrix} = \begin{bmatrix} \mathbf{Y^{GG}} & \mathbf{Y^{GL}} \\ \mathbf{Y^{LG}} & \mathbf{Y^{LL}} \end{bmatrix} \begin{bmatrix} \mathbf{V^G} \\ \mathbf{V_L} \end{bmatrix} \tag{3.2}$$

$$\mathbf{I^G = Y^{GG}V^G + Y^{GL}V^L} \tag{3.3}$$

$$\mathbf{I^L = Y^{LG}V^G + Y^{LL}V^L} \tag{3.4}$$

After performing further mathematical manipulations, Eq. (3.2) can be reformulated and expressed as Eq. (3.5) to (3.7).

$$\mathbf{V^L = [Y^{LL}]^{-1} I^L - [Y^{LL}]^{-1} Y^{LG} V^G} \tag{3.5}$$

$$\mathbf{I^G = Y^{GL}[Y^{LL}]^{-1} I^L + (Y^{GG} - Y^{GL}[Y^{LL}]^{-1} Y^{LG}) V^G} \tag{3.6}$$

As a result, Eq. (3.5) and (3.6) can be expressed in matrix form.

$$\begin{bmatrix} \mathbf{V^L} \\ \mathbf{I^G} \end{bmatrix} = \begin{bmatrix} \mathbf{[Y^{LL}]^{-1}} & \mathbf{-[Y^{LL}]^{-1} Y^{LG}} \\ \mathbf{Y^{GL}[Y^{LL}]^{-1}} & \mathbf{Y^{GG} - Y^{GL}[Y^{LL}]^{-1} Y^{LG}} \end{bmatrix} \begin{bmatrix} \mathbf{I^L} \\ \mathbf{V^G} \end{bmatrix} \tag{3.7}$$

By rearranging the aforementioned matrix, we obtain:

$$\begin{bmatrix} \mathbf{V^L} \\ \mathbf{I^G} \end{bmatrix} = \begin{bmatrix} \mathbf{Z^{LL}} & \mathbf{F^{LG}} \\ \mathbf{K_{GL}} & \mathbf{Y^{GG}} \end{bmatrix} \begin{bmatrix} \mathbf{I^L} \\ \mathbf{V^G} \end{bmatrix} \tag{3.8}$$

$$\mathbf{F_{LG} = -Y_{LL}{}^{-1} Y_{LG}} \tag{3.9}$$

$$L_j = \left| 1 - \sum_{i=1}^{i=g} F_{ij} \frac{V_i}{V_j} \right| \tag{3.10}$$

Before calculating the L-Index, the voltage values for each system bus and the Y-bus admittance matrix must be determined using the Newton-Raphson Load Flow (NRLF) approach. Finally, the required matrix is obtained by converting it from the Y-bus. The L-Index value is then computed using Eq. (3.10). It should be emphasized that the L-Index is solely determined for loaded buses. Furthermore, an L-Index value around 1 implies that the related bus is the weakest, which could result in a voltage collapse in the system. In contrast, a bus with an L-Index value near to zero is considered to be the most reliable.

3.3 P-V curve

The P-V curve, or Power-Voltage curve, is a graphical tool used to show how the voltage at a specific bus change as the real power (P) supplied to that bus increases. To create this curve, the load at the chosen bus gradually increased in small steps. After each increase, a load flow calculation is performed to determine the new voltage at that bus. This process continues until the load flow calculation can no longer find a solution, which indicates the system has reached its stability limit or is about to experience voltage collapse. The calculation can be done according to the graph details as fig. 3.1.

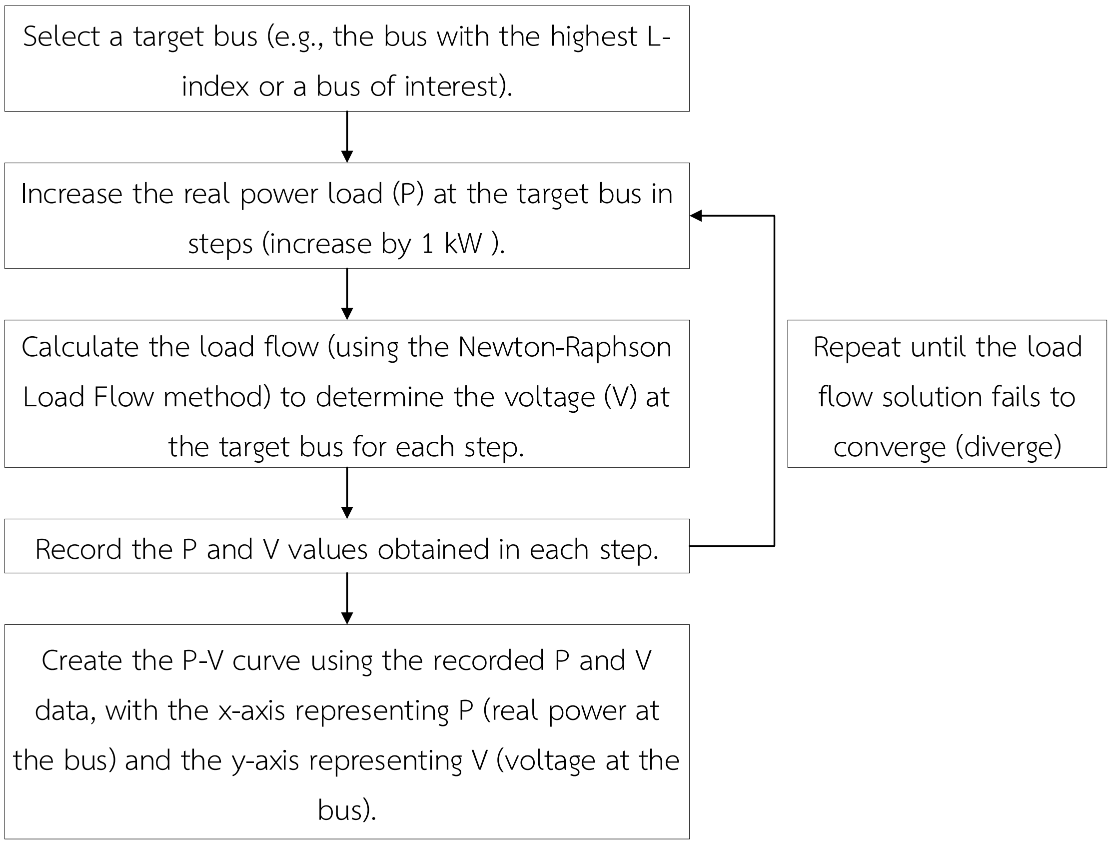

Figure 3.1 PV curve procedure

3.4 Voltage Stability Improvement Using PSO

PSO is a well-known metaheuristic algorithm inspired by birds' flocking behavior during food looking for. It iteratively explores the solution space by altering particle positions, integrating individual and shared experiences to determine the personal and global optimal positions. This technique incorporates velocity updates and seeks to arrive at a perfect solution.

PSO has emerged as a promising approach to improving voltage stability in microgrid systems. It accomplishes this by identifying the best generator bus voltages to reduce the L-index, a key indicator of the voltage stability margin. PSO's inherent characteristics such as its simplicity, computational efficiency, and adaptability make it appropriate for this application.

The fitness function that minimizes the L-index value of the weakest bus can be mentioned as,

$$\text{minimize } f(x_i^t) = \max\{\text{L-index}\}, \quad (3.11)$$

The computation of velocity and position is performed using the following equations:

$$v_i^{t+1} = wv_i^t + c_1 r_1 (pBest_i^t - x_i^t) + c_2 r_2 (gBest^t - x_i^t) \quad (3.12)$$

$$x_i^{t+1} = x_i^t + v_i^t \quad (3.13)$$

In this case, the population of particles reflects the generator voltage values. The generator voltage is listed as 0.95 and 1.05 per unit, respectively. Fig 3.2 depicts the proposed PSO-based computational approach for improving VSI.

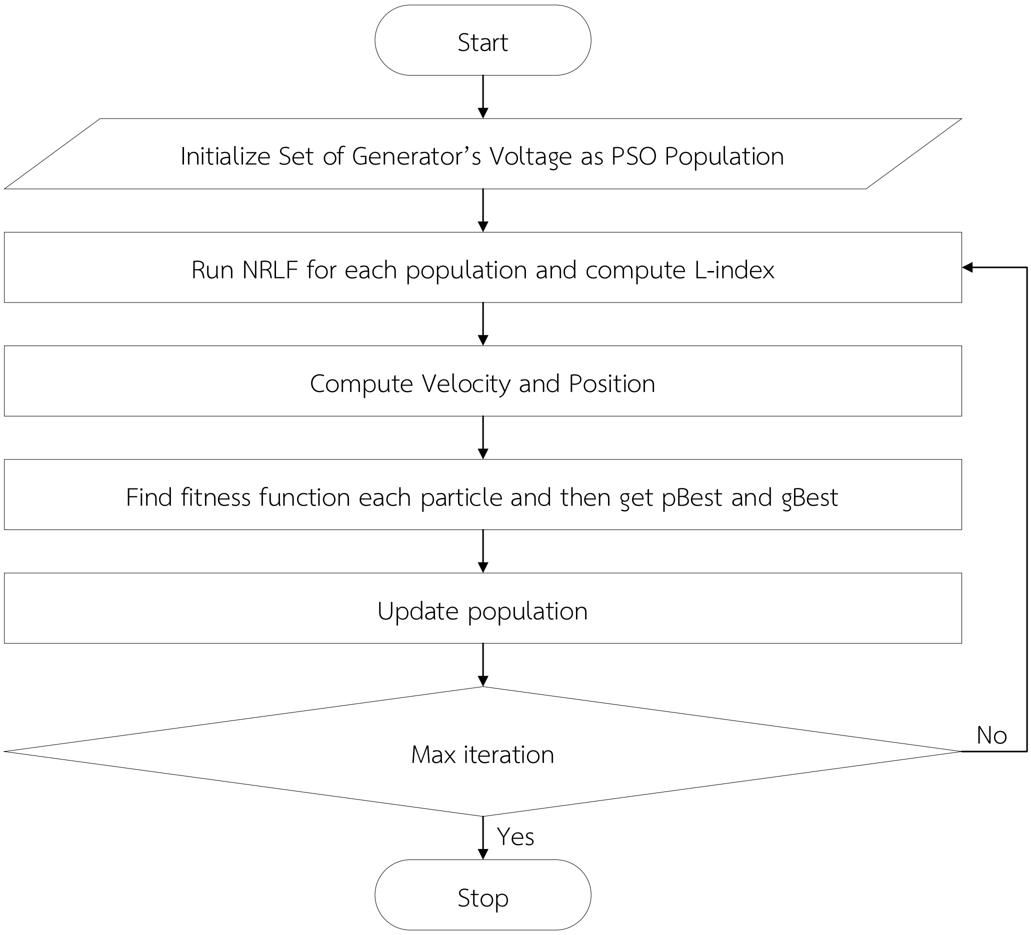

Figure 3.2 Computation Procedure

3.5 Results and Discussion

This section presents the results of the proposed method applied to the IEEE 33-bus distribution system. The analysis is segmented into four distinct cases, which are detailed below.

- IEEE 33-bus base case
- IEEE 33-bus with L-index improvement
- IEEE 33-bus modified
- Modified IEEE 33-bus system with L-index improvement

3.5.1 IEEE 33-bus base case

Figure 3.3 depicts the base case of the IEEE 33-bus system, which consists of one slack bus and 32 load buses, with the slack bus voltage set to 1.0 per unit (p.u.). Fig 3.4 shows the L-Index values calculated for each bus in the system. Bus 18 has the greatest L-Index value, making it the weakest bus in the network. Bus 2 has the lowest L-Index value, indicating it is the strongest bus. Bus 18's elevated L-Index value indicates a significant susceptibility to voltage collapse in the system. Furthermore, Fig 3.5 depicts the PV curve for Bus 18, demonstrating that voltage collapse occurs when the real power loading hits 2,672 kW.

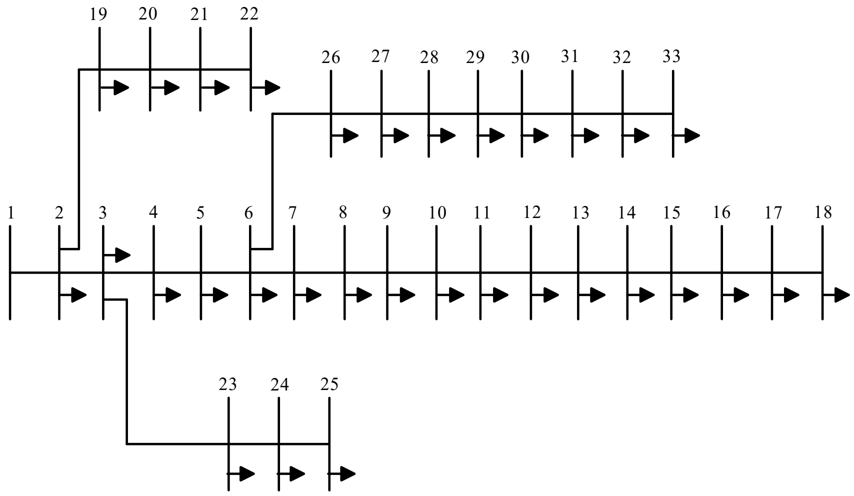

Figure 3.3 IEEE 33-bus system

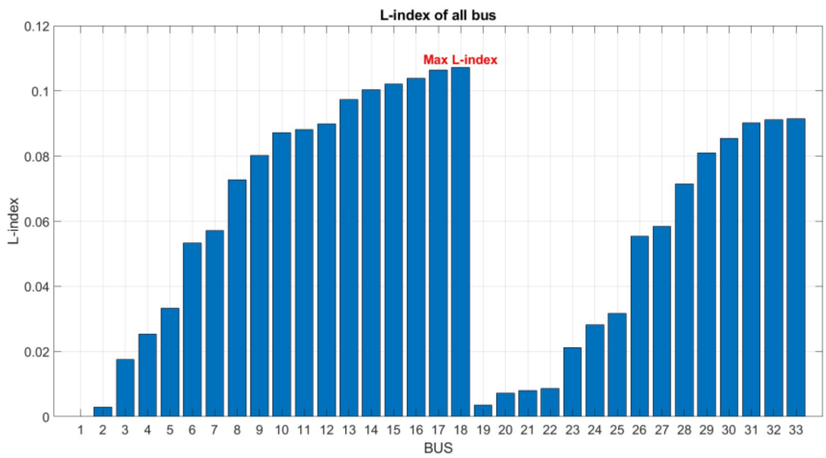

Figure 3.4 L-index of IEEE 33-bus base case

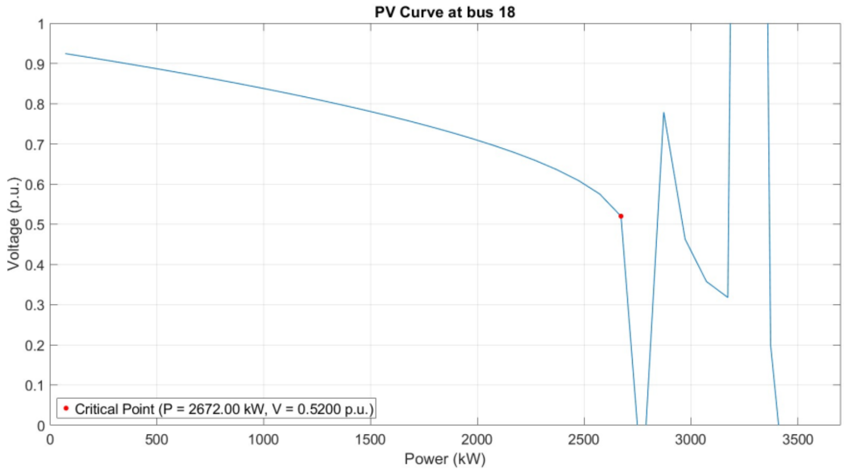

Figure 3.5 PV-curve of IEEE 33-bus base case

3.5.2 IEEE 33-bus with L-index improvement

Using the proposed method, the best generator voltage at the slack bus is calculated to be 1.05 per unit. Figure 3.6 demonstrates that in this improved system, the L-index values have decreased. Bus 18 is the weakest bus, while Bus 2 remains the strongest in the network. However, when compared to the prior scenario, the buses' L-index values are significantly lower. Figure 3.7 depicts the PV curve of the modified system, which shows that Bus 18's maximum loading capability has increased to 3,072 kW.

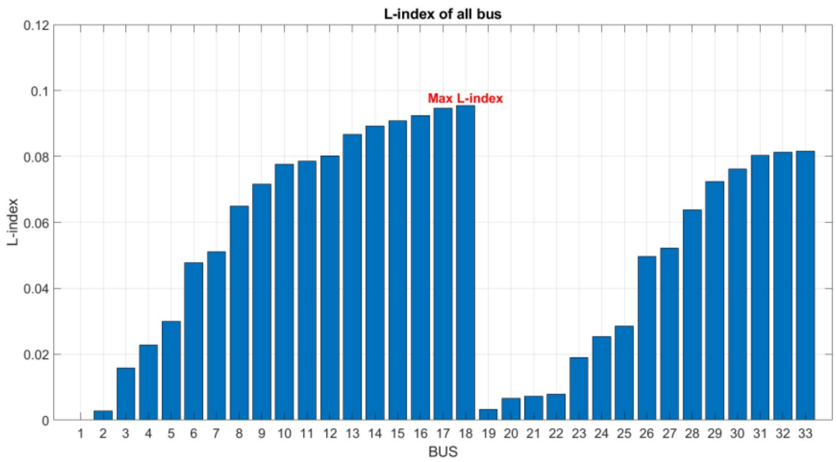

Figure 3.6 L-index of IEEE 33-bus with L-index improvement

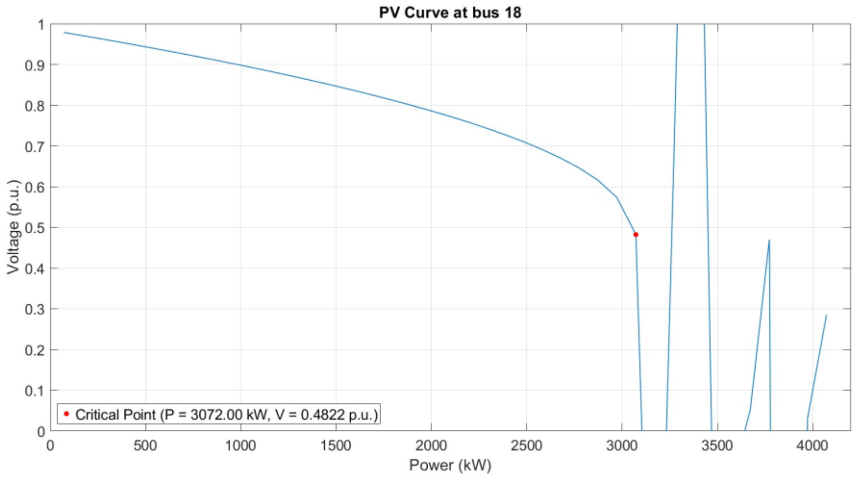

Figure 3.7 PV-curve of IEEE 33-bus system with L-index improvement

3.5.3 IEEE 33-bus modified

In this case, the IEEE 33-bus system is modified by installing four distributed generators (DGs) at buses 18, 22, 25, and 31, with power outputs of 1.075 MW, 0.36 MW, 0.93 MW, and 0.92 MW, respectively. The locations for DG installation are selected based on the lowest L-index value in each branch, while the DG capacities are determined according to the total power demand of each branch. For the microgrid (MG) case study, Bus 1 is disconnected from the main power grid. The voltage at all generator buses is set to 1 p.u., and Bus 18 is designated as the slack bus, as illustrated in Fig. 3.8.

Figure 3.9 shows the L-index of the modified IEEE 33-bus, similarly Bus 8 is a weaker bus, while bus 17 is a stronger bus. As observed, the weak bus is the farthest bus from the power sources. On the other hand, the strong bus is the nearest to the power sources. Fig 3.10 shows the PV-curve of bus 8, The maximum loading capability is 1,100 kW.

From table 3.1, in the base case, the voltage magnitude at bus 1 is set to 1.0 per unit, resulting in a maximum L-index of 0.1072 and a power output at the slack bus of 3.926 MW. After applying PSO, the voltage magnitude increases at bus 1 to 1.05 per unit, the maximum L-index is reduced to 0.0954, indicating an improvement in voltage stability. Additionally, the power at the slack bus slightly decreases to 3.9035 MW.

This demonstrates that optimizing the voltage magnitude using PSO can effectively reduce the maximum L-index, thereby enhancing the voltage stability of the system. The slight reduction in power at the slack bus also suggests a more efficient power flow, as losses may be reduced. Overall, the results confirm that the proposed method can improve system stability with minimal impact on the overall power supplied by the slack bus.

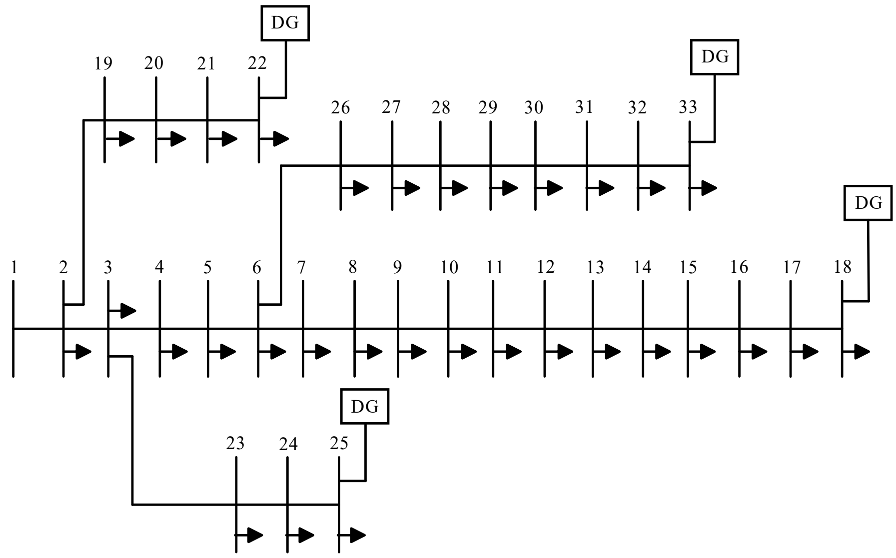

Figure 3.8 Modified IEEE 33-bus system

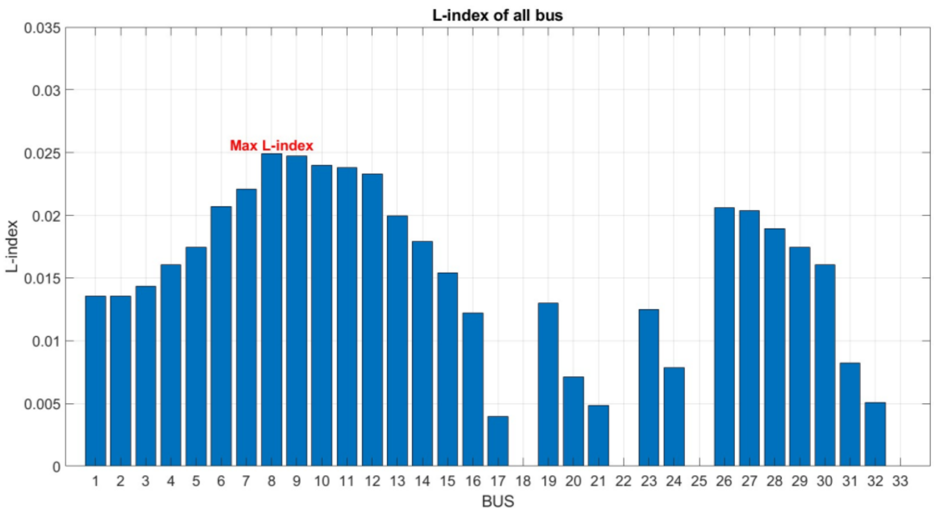

Figure 3.9 L-index of modified IEEE 33-bus.

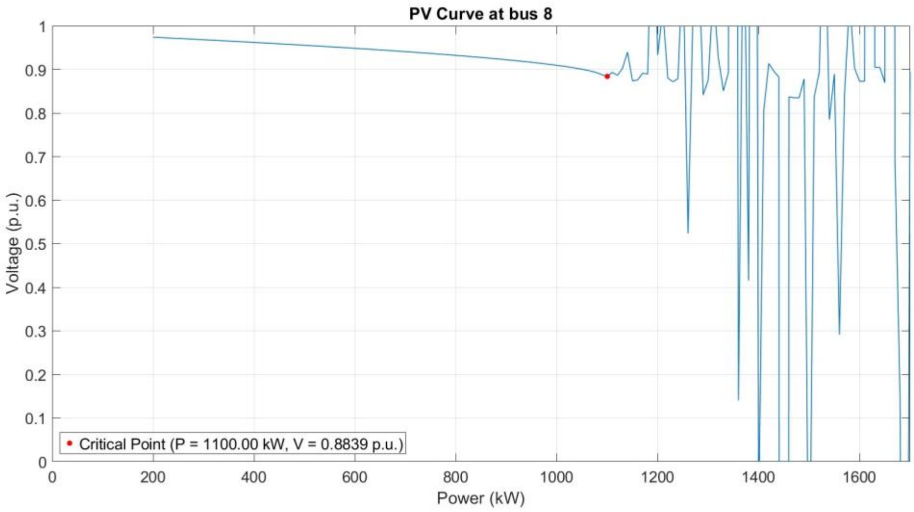

Figure 3.10 PV-curve of modified IEEE 33-bus.

Table 3.1 Comparison of IEEE 33-bus Base Case and L-index Improvement Results

Case	Bus	Voltage Magnitude	Max L-index	Power at Slack Bus (MW)
IEEE 33-bus base case	1	1	0.1072	3.926
IEEE 33-bus with L-index improvement	1	1.05	0.0954	3.9035

3.5.4 Modified IEEE 33-bus system with L-index improvement

In this case, PSO is used to find the optimal solution for the objective, which is to minimize the maximum L-index of the buses. The optimization is performed by adjusting the voltage levels of generator buses or designated buses, with the voltage search space constrained within the standard voltage limits of 0.95 to 1.05 p.u. The test is conducted on a modified power system, based on the same configuration as Case 3, making the system under study effectively resemble a microgrid.

Figure 3.11 depicts the L-index values for each bus of the modified IEEE 33-bus system. When compared to previous cases, L-index values are significantly lower, indicating that voltage stability has improved. Bus 8 is established as a weak bus, whereas Bus 17 remains the strongest bus in the network.

Figure 3.12 shows the PV curve for the improved IEEE 33-bus system following the L-index optimization. The investigation shows that the system's maximum loading capacity has increased to 1,260 kW, indicating its ability to handle higher loading levels. This increase in loading capacity shows the system's increased stability, demonstrating the successful result of the proposed optimization strategy in reinforcing voltage stability.

Table 3.2 presents a comparison between the IEEE 33-bus Modified case and the case where the L-index is improved by increasing the voltage magnitude at buses 18, 22, 25, and 33 from 1.00 pu to 1.05 pu.

In the base case, where the voltage magnitude at these four buses is set to 1.00 pu, the maximum L-index is 0.0249, and the power at the slack bus is 3.2596 MW. After increasing the voltage magnitude at buses 18, 22, 25, and 33 to 1.05 pu, the maximum L-index decreases to 0.0225, indicating an improvement in voltage stability. Additionally, the power at the slack bus slightly decreases to 3.2354 MW, suggesting a reduction in system losses and a more efficient power supply.

These results demonstrate that optimizing the voltage magnitude at selected buses can effectively reduce the maximum L-index, thereby enhancing the voltage stability of the system. The slight reduction in slack bus power also indicates improved system efficiency. Overall, the proposed method improves system stability without negatively impacting the overall power supply.

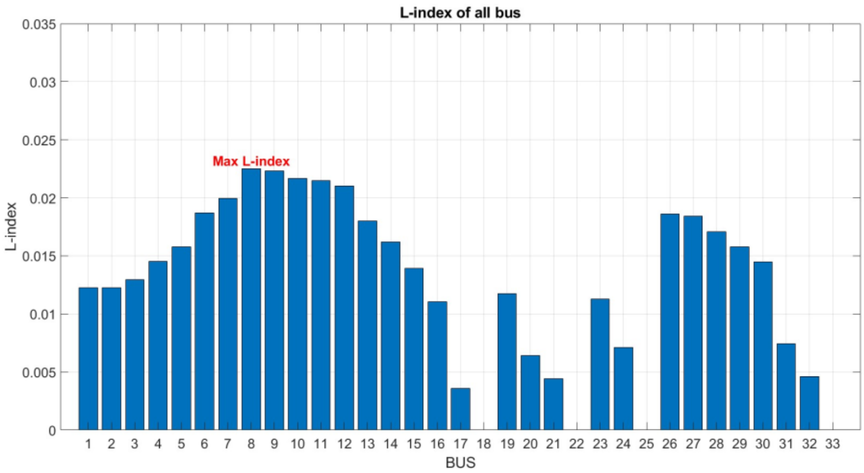

Figure 3.11 L-index of modified IEEE 33-bus system with L-index improvement.

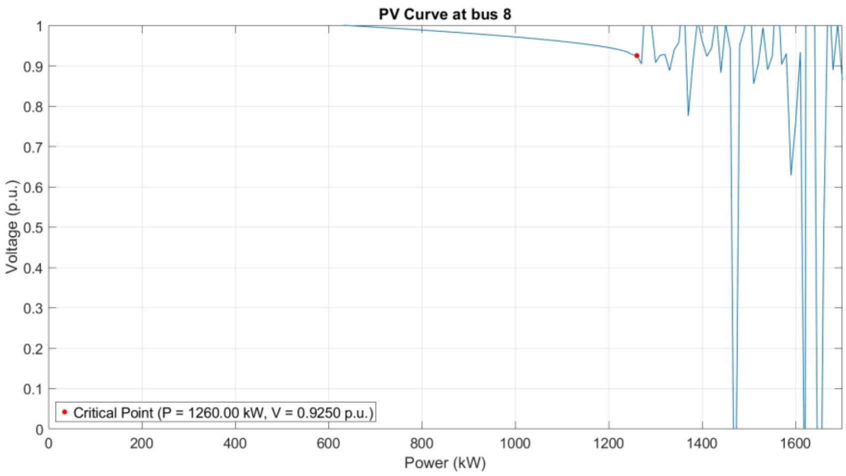

Figure 3.12 PV-curve of modified IEEE 33-bus system with L-index improvement.

Table 3.2 Comparison of IEEE 33-bus Modified Case and Modified IEEE 33-bus system with L-index improvement Results

Case	Bus	Voltage Magnitude	Max L-index	Power at Slack Bus (MW)
IEEE 33-bus Modified	18	1.00	0.0249	3.2596
	22	1.00		
	25	1.00		
	33	1.00		

Table 3.2 Comparison of IEEE 33-bus Modified Case and Modified IEEE 33-bus system with L-index improvement Results (Continued)

Case	Bus	Voltage Magnitude	Max L-index	Power at Slack Bus (MW)
Modified IEEE 33-bus system with L-index improvement	18	1.05	0.0225	3.2354
	22	1.05		
	25	1.05		
	33	1.05		

Table 3.3 demonstrates that the system's voltage stability has improved, as indicated by the lower L-Index values. The reduction in L-Index values significantly enhances system stability during the optimization process. It is important to note that the table does not include L-Index values for PV buses, since the L-Index calculation is only applicable to load buses. In the IEEE 33-bus base case, Bus 1 is identified as a PV bus, while in the modified IEEE 33-bus system, Buses 18, 22, 25, and 33 are classified as PV buses.

When analyzing system stability, it is evident that in the base case, Bus 18 consistently exhibits the highest L-Index value, followed by Buses 17, 16, and 15. This suggests that Bus 18 is the least reliable and has the greatest potential to contribute to system instability. In the modified IEEE 33-bus system, Bus 8 has the highest L-Index value, indicating similarly low reliability. If an abnormal event occurs, there is a high likelihood that voltage collapse would originate from this bus.

Therefore, to ensure system stability, special attention should be given to Bus 18 in the base case and Bus 8 in the modified case. Improving the operational conditions of these buses is crucial for maintaining the overall stability of the IEEE 33-bus system.

Additionally, the PV curves indicate that the modified IEEE 33-bus system achieves the highest level of stability, as it can accommodate a greater load capacity compared to the other cases analyzed. This improvement highlights the effectiveness of the proposed optimization strategy in enhancing voltage stability within the system.

Table 3.3 Comparing L-index value

BUS	L-index			
	IEEE 33-bus base case	IEEE 33-bus with L-index improvement	IEEE 33-bus Modified	IEEE 33-bus Modified with L-index improvement
1	-	-	0.013538	0.012246
2	0.003004	0.002708	0.013538	0.012246
3	0.017498	0.015742	0.014334	0.012964
4	0.025411	0.022832	0.016056	0.014515
5	0.033364	0.029944	0.017475	0.015794
6	0.053276	0.047698	0.020685	0.018688
7	0.057172	0.051161	0.022083	0.019952
8	0.072771	0.064999	0.024913	0.022498
9	0.080183	0.071556	0.024711	0.022318
10	0.087129	0.077691	0.023974	0.021655
11	0.088143	0.078586	0.023783	0.021484
12	0.089917	0.080151	0.023296	0.021046
13	0.097415	0.086758	0.01994	0.018023
14	0.100304	0.089300	0.017937	0.016216
15	0.102096	0.090877	0.015424	0.013949
16	0.103813	0.092386	0.012216	0.011053
17	0.10646	0.094713	0.003944	0.003572
18	0.107227	0.095386	-	-
19	0.003527	0.003181	0.013009	0.011769
20	0.00723	0.006535	0.007095	0.006424

Table 3.3 Comparing L-index value (Continued)

BUS	L-index			
	IEEE 33-bus base case	IEEE 33-bus with L-index improvement	IEEE 33-bus Modified	IEEE 33-bus Modified with L-index improvement
21	0.007993	0.007225	0.004864	0.004405
22	0.008698	0.007864	-	-
23	0.021172	0.019053	0.012484	0.011293
24	0.028149	0.025332	0.007876	0.00713
25	0.031696	0.028521	-	-
26	0.055454	0.049636	0.020612	0.018622
27	0.058377	0.052235	0.020373	0.018407
28	0.071425	0.063818	0.018922	0.017099
29	0.081028	0.072323	0.01744	0.015762
30	0.085367	0.076160	0.016048	0.014506
31	0.090123	0.080360	0.008235	0.007452
32	0.091174	0.081288	0.005073	0.004592
33	0.091500	0.081576	-	-

From the comparison table 3.4 of the 33-bus distribution system under different scenarios, the base case, L-index improvement, network modification, and network modification combined with L-index improvement it is evident that both L-index and network improvements have a significant impact on system performance.

In the base case, the system exhibits a total power loss of 0.2110 MW and a power supply from the slack bus of 3.926 MW. When the L-index improvement is applied, the power loss decreases to 0.1804 MW, and the power supplied by the slack bus is reduced to 3.2596 MW. This demonstrates that L-index improvement can significantly reduce system losses and enhance the efficiency of power delivery.

In the Modification case, when both network modification and L-index improvement are applied together, the results are optimal. The power loss is minimized to 0.1804 MW, and the slack bus power is reduced to 3.2596 MW, which is the lowest value among all studied cases.

Additionally, the total generation power required tends to decrease as the system is improved, reflecting a reduction in system losses and overall energy savings.

Based on these results, it can be concluded that the combination of L-index and network improvements provides the highest efficiency for the distribution system. This approach effectively reduces power losses and the burden on the slack bus, thereby enhancing the overall performance of the power distribution network.

Table 3.4 Comparison Real Power All Cases

Case	Total Power Loss (MW)	Total Power Load (MW)	Power at Slack Bus (MW)	Total Generation Power (MW)
IEEE 33-bus base case	0.211	3.715	3.926	3.926
IEEE 33-bus with L-index improvement	0.1885	3.715	3.9035	3.9035
IEEE 33-bus modified	0.2046	3.055	1.6196	3.2596
Modified IEEE 33-bus system with L-index improvement	0.1804	3.055	1.5954	3.2354

3.6 Chapter Summary

This chapter demonstrates that improving both the L-index and the network configuration in the IEEE 33-bus distribution system can greatly enhance the system’s overall performance. By applying these two strategies together, the system experiences the lowest power losses and the least burden on the slack bus compared to all other scenarios studied. This means that not only is the system more efficient, but it also saves more energy overall.

A key finding is that certain buses specifically Bus 18 in the original system and Bus 8 in the modified system are the most vulnerable points in terms of voltage stability. These buses have the highest L-index values, which makes them the most likely spots for voltage instability or even collapse if something goes wrong. Therefore, focusing on improving the conditions at these buses is essential for keeping the whole system stable.

The chapter also highlights the results from the PV-curve analysis, which shows that the L-index improvement can handle a higher load before reaching its stability limit. This is a clear sign that the proposed optimization methods are effective at making the system more robust.